Uncertainty Analysis for Steady-state Inviscid Burgers' Equation

Q. Chen[†], D. Gottlieb[†], and J. S. Hesthaven[†]

Abstract

It is well known that the steady state of an isentropic flow in a dual-throat nozzle with equal throat areas is not unique. In particular there is a possibility that the flow contains a shock wave, whose location is determined by the initial condition. We consider, in this paper, the case in which there is uncertainty concerning the initial condition and use generalized polynomial chaos methods to study the steady-state solutions for stochastic initial conditions, with special interest focused on the statistics of the shock location.

The polynomial chaos (PC) expansion modes are shown to be smooth functions of the spatial variable x, although each solution realization is discontinuous in the spatial variable x.

When the variance of the initial condition is small, the probability density function (PDF) of the shock location is computed with high accuracy. Otherwise, many terms are needed in the PC expansion to produce reasonable results due to the slow convergence of the PC expansion, caused by the non-smoothness in the random space.

[†]Division of Applied Mathematics, Brown University, Box F, Providence, RI 02912 (cqy@cfm.brown.edu, dig@cfm.brown.edu, jansh@cfm.brown.edu).

1 Introduction

In [11] a model for the isentropic flow in a dual-throat nozzle with equal throat areas was considered. The steady state flow can be either completely supersonic or completely subsonic or a flow containing a shock wave connecting the supersonic branch of the solution to the subsonic branch. The location of the shock wave depends uniquely on the initial condition (see also [3]). The question arises: what can be said about the shock location if there are uncertainties in the initial conditions. While randomness enters through the initial conditions in this problem, random effects can generally enter into practical problems through boundary conditions, initial conditions, the domain geometry, missing variables and fluid properties etc. ([10, 7, 17]). Such random effects in the inputs produce stochastic solutions as outputs, requiring new methodologies to model and analyze the impact of such uncertainties.

In our case we are interested in the statistics of some derived quantities (e.g., the shock position of a solution). Such are often hard to accurately compute from the first few moments of the solutions. We demonstrate this point with the following diagram (1). Here $\boldsymbol{\xi}$ is a vector of random variables. $\mu(x)$ and $\sigma(x)$ denote the mean and standard variation of $u(x,\boldsymbol{\xi})$, respectively. $X_s(\boldsymbol{\xi})$ is the shock location of $u(x,\boldsymbol{\xi})$. μ_{X_s} and σ_{X_s} are the first two moments of X_s.

$$\begin{array}{rcccc} & u(x,\boldsymbol{\xi}) & \xrightarrow{\text{Statistics}} & \{\mu(x),\sigma(x),\cdots\} & \\ \text{Locating Shock} & \downarrow & & \downarrow ?? & \\ & X_s(\boldsymbol{\xi}) & \xrightarrow{\text{Statistics}} & \mu_{X_s},\sigma_{X_s},\cdots & \end{array} \quad (1)$$

In most practical situations, the deterministic and probabilistic parts of $u(x,\boldsymbol{\xi})$ can not be separated (i.e., $u(x,\boldsymbol{\xi})$ can not be written into the form $u(x,\boldsymbol{\xi}) = f(x)g(\boldsymbol{\xi})$). So the shock locating procedure and statistics computation procedure do not commute with each other because of the complexity and nonlinearity of the former. Therefore there is generally no easy way to accurately compute μ_{X_s} and σ_{X_s} from the first few components of $\{\mu(x),\sigma(x),\cdots\}$.

When additional information is being required about the solution, series expansion methods ([12, 14, 7]) appear as a choice for the discretization of random fields. Moreover, the correlation function of the solution is often unknown *a priori*, therefore generalized polynomial chaos methods seem to be suitable in this scenery. Recall that Chorin showed ([2]) that using those methods is limited to large scale hydrodynamical problems, since the small scales are not Gaussian.

In this paper, we study the model equation of the isentropic flow in a dual-throat nozzle with equal throat areas introduced in [11]. Generalized polynomial chaos methods are implemented to compute the probability density function (PDF) of the shock location for the cases where the initial conditions are assumed to be different random processes (fields). When exact solutions are not available, we use the basic Monte Carlo method to validate the results.

The rest of the paper is organized as follows. In Sec. 2, we recall the basic Monte Carlo (MC) method and generalized polynomial chaos methods. We also discuss boundary conditions issues for the system obtained when introducing the polynomial chaos expansion. Section 3 includes results from the MC method, Hermite and Jacobi polynomials chaos methods for the model equation. The polynomial chaos expansion is shown to converge slowly for functions which are discontinuous in the random space as already shown in [2]. Finally, we summarize the results of the paper in Sec. 4.

2 Monte Carlo Method and Generalized Polynomial Chaos Methods

In this section, we offer a short review of the basic Monte Carlo method ([17]) and generalized polynomial chaos ([5, 18]) methods. We also discuss the issues of boundary conditions for hyperbolic equations.

2.1 Monte Carlo Method

In the basic Monte Carlo method, one generates a number of samples of the input stochastic processes, solves the deterministic equations for each sampled input, and computes the statistics of the desired variables from the solutions. One advantage of Monte Carlo methods is that we only need to execute the code for the deterministic problems with the sampled inputs. It can provide accurate solutions as long as the number of samples is high enough. The major drawback is the large amount of computing time it requires when the standard variation of the output is not small, a particular problem when higher moments are more interested. Importance sampling and correlation methods can be used to substantially improve the efficiency for certain problems. One can consult the literature [12], [17] and references therein for more information on advanced applications of Monte Carlo methods.

2.2 Generalized Polynomial Chaos Methods

Generalized polynomial chaos ([18, 5]) methods involve a spectral representation of the stochastic processes (random functions). In particular, stochastic processes are expanded into multi-dimensional orthogonal generalized hypergeometric polynomials ([1]) of identical independent (*iid*) random variables $\boldsymbol{\xi}$. For a specific random process, the corresponding hypergeometric polynomials should be used to achieve optimal accuracy with a minimum number of expansion terms, e.g., Hermite polynomials should be used for Gaussian processes, and Jacobi polynomials should be used for Beta processes (See [18] for a complete list).

Generalized hypergeometric polynomials form a complete orthogonal basis of the L_2 space of random variables. The weighted inner product is defined as

$$< f(x,\boldsymbol{\xi}),\ g(x,\boldsymbol{\xi}) > \ = \int f(x,\boldsymbol{\xi})g(x,\boldsymbol{\xi})\omega(\boldsymbol{\xi})d\boldsymbol{\xi} \ = \ E[f(x,\boldsymbol{\xi})g(x,\boldsymbol{\xi})] \ ,$$

where the weight function $\omega(\boldsymbol{\xi})$ is the joint probability density function (PDF) of the random variables. In particular, for the n-dimensional Gaussian random variables, $\boldsymbol{\xi}$,

$$\omega(\boldsymbol{\xi}) = \frac{1}{\sqrt{(2\pi)^n}} e^{-\frac{1}{2}\boldsymbol{\xi}^T\boldsymbol{\xi}}. \tag{2}$$

As an example, a Gaussian process $u(x,\theta)$ (with x being the spatial or time coordinate) is expanded as

$$u(x,\theta) = \sum_{l=0}^{+\infty} u_l(x)\psi_l(\boldsymbol{\xi}(\theta)) \ , \tag{3}$$

where $\boldsymbol{\xi}(\theta)$ is a vector of *iid* Gaussian random variables with zero mean and unit variance, and the basis functions $\psi_l(\boldsymbol{\xi}(\theta))$ are the normalized (multidimensional) Hermite polynomials given by

$$H_{(n,p)}(\xi_{i_1},\cdots,\xi_{i_p}) = e^{\frac{1}{2}\boldsymbol{\xi}^T\boldsymbol{\xi}}(-1)^p \frac{\partial^p}{\partial\xi_{i_1}\cdots\partial\xi_{i_p}}\left(e^{-\frac{1}{2}\boldsymbol{\xi}^T\boldsymbol{\xi}}\right), \qquad \forall \quad 1 \le i_1,\cdots,i_p \le n \ .$$

In the computations we use the p-th order approximation:

$$u_P(x,\theta) = \sum_{l=0}^{P} u_l(x)\psi_l^{(n)}(\boldsymbol{\xi}(\theta)) \ , \tag{4}$$

where $P = \frac{(n+p)!}{n!p!}$, $\boldsymbol{\xi}(\theta) = (\xi_1(\theta)\ ,\cdots,\ \xi_n(\theta))^T$.

The superscript of $\psi_l^{(n)}$ will be omitted if there is no confusion. Note that there is only one zeroth degree PC basis function $\psi_0(\boldsymbol{\xi}) = 1$.

Since $\{\psi_i(\boldsymbol{\xi})\}$ form an orthonormal basis, the PC expansion coefficients of $u(x,\boldsymbol{\xi})$ are given by

$$u_l(x) \ = < u(x,\boldsymbol{\xi}),\ \psi_l(\boldsymbol{\xi}) > \ \ = E[u(x,\boldsymbol{\xi})\psi_l(\boldsymbol{\xi})]. \tag{5}$$

It is easy to verify that the mean of $u(x,\boldsymbol{\xi})$ is the zero mode $u_0(x)$, and the variance is $VAR(u(x,\boldsymbol{\xi})) = \sum_{i=1}^{+\infty}(u_i(x))^2$. Moreover, one can generate any number of realizations of $u(x,\boldsymbol{\xi})$ by sampling in $\boldsymbol{\xi}$. This makes it possible to compute the statistics of any derived quantity of the solutions when $\{u_i\}$ are known.

2.2.1 Karhunen Loève Expansion

The Karhunen Loève (KL) expansion ([9]) is another spectral representation of random processes. For any random process $u(x,\theta)$ with x as the spatial or time coordinates defined over the domain D, the KL expansion takes the form

$$u(x,\theta) = \bar{u}(x) + \sum_{k=1}^{+\infty} \sqrt{\lambda_k}\; f_k(x)\boldsymbol{\xi}_k(\theta) \; , \tag{6}$$

where $\{\boldsymbol{\xi}_k(\theta)\}$ is a set of uncorrelated random variables with zero mean and unit variance. $\bar{u}(x)$ is the mean of $u(x,\theta)$; λ_k and $f_k(x)$ are the k^{th} eigenvalue and eigenfunction of the covariance function $C(x_1,x_2)$ of $u(x,\boldsymbol{\xi})$, i.e.,

$$\int_D C(x_1,x_2) f_k(x_1) dx_1 = \lambda_k f_k(x_2) \; . \tag{7}$$

The Karhunen Loève (KL) expansion is optimal among all possible representations of random processes in the sense of the mean-square error. But its use is limited because the covariance function of the solution in many problems is *a priori* unknown. Even if known, (7) may be expensive to solve. It has been used to discretize the input random processes by many authors ([18, 5]) in order to determine the dimension of the polynomial chaos approximations of the solution process.

2.2.2 Implementation and Boundary Conditions for Hyperbolic Equations

A sensitive issue in the application of PC methods to hyperbolic equations is the implementation of boundary conditions. The PC method leads to a system of equations for the expansion coefficients. This system should remain well posed and in particular should not require boundary conditions at the outflow of the original problem.

Consider the scalar linear hyperbolic equation

$$u_t + a(x,t,\boldsymbol{\xi})\; u_x = 0, \qquad 0 \le x \le \pi, \quad t > 0 \; , \tag{8}$$

where $a(x,t,\boldsymbol{\xi})$ depends on a random vector $\boldsymbol{\xi}$.

We represent the solution as in (4) and also expand $a_P(x,t,\boldsymbol{\xi}) = \sum_{l=0}^{P} a_l(x,t)\psi_l(\boldsymbol{\xi})$. A standard Galerkin procedure yields the system

$$\frac{\partial u_k}{\partial t} + \sum_{i,j=0}^{P} a_i e_{ijk} \frac{\partial u_j}{\partial x} = 0 \qquad k = 0, \cdots, P \;, \tag{9}$$

where

$$e_{ijk} = E[\psi_i \psi_j \psi_k] \quad ,$$

or in matrix form

$$\vec{U}_t + A\, \vec{U}_x = 0 \quad , \tag{10}$$

where $\vec{U} = (u_0(x,t), \cdots, u_P(x,t))^T$ and the matrix $A = (A_{i,j})$ has elements

$$A_{i,j} = \sum_{l=0}^{P} a_l e_{ijl} \qquad , \qquad 0 \le i,j \le P \quad .$$

Thus, the scalar equation (8) for the random function $u(x,t,\boldsymbol{\xi})$ is transformed to the system (10) of several deterministic unknowns: $\{u_0(x,t), \cdots, u_P(x,t)\}$. We can determine the nature of the system:

Theorem 1 *The system* (10) *is symmetric hyperbolic . Moreover, if* $a_P(x,t,\boldsymbol{\xi}) \ge (\le)\ 0$ *for all* $\boldsymbol{\xi}$ *at a point* (x,t)*, then* $A \ge (\le)\ 0$*, at this point.*

Proof: The symmetry of the matrix A follows directly from the definition of (e_{ijl}).

Given any real vector $b = (b_0, \cdots, b_P)$,

$$\begin{aligned} b\ A\ b^T &= \sum_{i,j=0}^{P} b_i A_{ij} b_j = \sum_{i,j=0}^{P} b_i b_j \sum_{l=0}^{P} a_l e_{ijl} = \sum_{l=0}^{P} a_l \sum_{i,j=0}^{P} b_i b_j e_{ijl} \\ &= \sum_{l=0}^{P} a_l \sum_{i,j=0}^{P} b_i b_j E[\psi_i \psi_j \psi_l] \\ &= E\left[\left(\sum_{l=0}^{P} a_l \psi_l \right) \left(\sum_{i=0}^{P} b_i \psi_i \right) \left(\sum_{j=0}^{P} b_j \psi_j \right) \right] \\ &= E[a_P(x,t,\boldsymbol{\xi}) \beta(x,t,\boldsymbol{\xi})^2] \end{aligned}$$

where $\beta(x,t,\boldsymbol{\xi}) = \sum_{i=0}^{P} b_i \psi_i$. From the last expression, the theorem follows. ■

Note that if the conditions in the theorem are fulfilled then the boundary conditions for the derived system (10) are consistent with the boundary condition of the approximation of the original equation (8).

2.3 Computation of a Smooth PDF

In this paper we adopt the (OSCM) method presented in [8], for computing a 'smooth' PDF of any random variable based on few samples. Assume that $f(x)$ is the PDF of a random variable at x, and $\{x_1, \cdots, x_N\}$ are N MC samples. Then $f(x)$ is the sum of δ-functions

$$f(x) = \frac{1}{N} \sum_{i=1}^{N} \delta(x - x_i) \; . \tag{11}$$

We note that

$$\delta(x - x_i) = \sum_{n=0}^{\infty} \frac{1}{\|P_n\|^2} P_n(x_i) P_n(x).$$

To regularize we take a finite sum

$$\sum_{n=0}^{K} \frac{1}{\|P_n\|^2} P_n(x_i) P_n(x),$$

which can also be expressed, using the Christoffel-Darboux formula, as:

$$\sum_{n=0}^{K} \frac{1}{\|P_n\|^2} P_n(x_i) P_n(x) = \frac{K+1}{2} \frac{P_{K+1}(x) P_K(x_i) - P_K(x) P_{K+1}(x_i)}{x - x_i}.$$

And finally,

$$\begin{aligned} f(x) \;&\sim\; \frac{1}{N} \sum_{i=1}^{N} \sum_{n=0}^{K} \frac{1}{\|P_n\|^2} P_n(x_i) P_n(x) \\ &= \frac{K+1}{2N} \sum_{i=1}^{N} \frac{P_{K+1}(x) P_K(x_i) - P_K(x) P_{K+1}(x_i)}{x - x_i}. \end{aligned} \tag{12}$$

3 Steady State Inviscid Burgers' Equation with Source Term

When an isentropic flow is choked in a dual-throat nozzle with equal throat areas, the steady flow can either be entirely supersonic, or subsonic, or contain a shock wave connecting the supersonic branch to the subsonic branch, depending on its initial state. In the latter case the shock location, is also determined by the initial state.

In [11] the following simplified model was analyzed:

$$\frac{\partial u}{\partial t} + \frac{\partial}{\partial x}\left(\frac{u^2}{2}\right) = \frac{\partial}{\partial x}\left(\frac{\sin^2 x}{2}\right) \qquad 0 \le x \le \pi, \quad t > 0 \tag{13}$$

with the initial condition

$$u(x, 0) = \beta \sin x, \tag{14}$$

and boundary conditions

$$u(0, t) = u(\pi, t) = 0.$$

The exact steady state solution to Eq. (13) is

$$u_\infty(x, \beta) = \lim_{t \to +\infty} u(x, \beta, t) = \begin{cases} u^+ = \sin x & 0 < x \le X_s \\ u^- = -\sin x & X_s < x < \pi \end{cases}, \tag{15}$$

The shock position X_s is a function of the parameter β in the initial condition:

$$X_s = \begin{cases} \sin^{-1}\left(\sqrt{1-\beta^2}\right) & < \pi/2 & -1 < \beta \le 0 \\ \pi - \sin^{-1}\left(\sqrt{1-\beta^2}\right) & > \pi/2 & 0 < \beta < 1 \end{cases}. \tag{16}$$

When $|\beta| \ge 1$, $u_\infty(x, \beta)$ is smooth ($= \text{sign}(\beta) \sin x$).

3.1 Inhomogeneous Random Initial Condition I: Hermite Chaos

Consider Eq. (13) with the initial condition

$$u(x, \beta, t = 0) = \beta \sin x \ , \tag{17}$$

where β is a *random variable* defined as

$$\beta = \begin{cases} \frac{-1+\sqrt{1+4\alpha^2}}{2\alpha} & \text{if } \alpha \neq 0 \\ 0 & \text{if } \alpha = 0 \end{cases} \qquad \text{or} \qquad \alpha = \frac{\beta}{1-\beta^2} \ . \tag{18}$$

Here α is a Gaussian random variable with the mean μ and standard variation σ, i.e., $\alpha \sim N(\mu, \sigma)$. The shock always exists in the steady state solution because β falls in $(-1, 1)$.

Note that the covariance function has the form

$$C(x_1, x_2) = VAR(\beta)\ \sin x_1\ \sin x_2\ , \qquad 0 \leq x_1, x_2 \leq \pi\ , \tag{19}$$

where $VAR(\beta)$ is the variance of β. Since it is not a function of $x_1 - x_2$ the initial condition is not a homogeneous random field ([19]).

From (16), one finds that $\beta = -\cos(X_s)$, i.e.,

$$\alpha = \frac{-\cos(X_s)}{(\sin X_s)^2}\ . \tag{20}$$

The PDF of the shock position X_s can therefore be computed directly:

$$\frac{1}{\sqrt{2\pi}\sigma} e^{-\frac{(\alpha-\mu)^2}{2\sigma^2}} d\alpha = p(X_s) dX_s \longrightarrow p(X_s) = \frac{1}{\sqrt{2\pi}\sigma} e^{-\frac{(\alpha-\mu)^2}{2\sigma^2}} \frac{d\alpha}{d\beta} \frac{d\beta}{dX_s}\ , \tag{21}$$

where $p(X_s)$ denotes the PDF of the shock position being at X_s. This yields

$$p(X_s) = \frac{1}{\sqrt{2\pi}\sigma} e^{-\frac{(\alpha-\mu)^2}{2\sigma^2}}\ \frac{1+\beta^2}{(1-\beta^2)^2}\ \sin(X_s)\ , \qquad 0 < X_s < \pi\ , \tag{22}$$

through $\beta = -\cos(X_s)$ and α as given by (20).

3.1.1 Hermite Polynomial Chaos Solution

Since β is a function of a single Gaussian random variable, α, a one-dimensional Hermite polynomial chaos approximation ($n = 1$) suffices to represent the random function $u_\infty(x, \beta(\xi))$, i.e., we consider the expansion:

$$u_\infty(x, \beta(\xi)) = \sum_{k=0}^{\infty} v_k(x) \psi_k(\xi) \tag{23}$$

In the next theorem we will establish that this expansion converges. Surprisingly, although $u_\infty(x, \xi)$ is not smooth in the spatial variable x, all the coefficients $v_k(x)$ are smooth.

Theorem 2 *(Smoothness) Let $u_\infty(x, \beta(\xi))$ be defined in (15). Let ξ is a Gaussian random variable with zero mean and unit variance and $\beta(\xi)$ is defined in (18). Then the expansion (23) converges and the coefficients $v_k(x)$ are smooth.*

Proof: From the relations between α, ξ, β and the shock position X_s, one finds

$$\xi = \frac{1}{\sigma}\left(\frac{-\cos X_s}{(\sin X_s)^2} - \mu\right) . \tag{24}$$

This implies that X_s is an increasing function of ξ and vice versa, as $0 < X_s < \pi$.

Let ξ_0 be the value of ξ which corresponds to the solution with shock position $x_0 \in (0, \pi)$, For a fixed x_0, the steady state solution of (13) is given by

$$u_\infty(x_0, \xi) = \begin{cases} -\sin(x_0(\xi_0)) & \text{if} \quad \xi \leq \xi_0 \\ \sin(x_0(\xi_0)) & \text{otherwise} \end{cases} . \tag{25}$$

Since the shock position is an increasing function of ξ, therefore,

$$\frac{1}{\sqrt{2\pi}} \int_{-\infty}^{+\infty} (u_\infty(x_0(\xi_0), \xi))^2 e^{-\frac{\xi^2}{2}} d\xi = (\sin x_0(\xi_0))^2 \ < +\infty , \tag{26}$$

and thus the expansion (23) convergence (see [4]).

The expansion coefficients are given by

$$\begin{aligned} v_k(x_0) &= \frac{1}{\sqrt{2\pi}} \int_{-\infty}^{+\infty} u_\infty(x_0(\xi_0), \xi) \ \psi_k(\xi) e^{-\frac{\xi^2}{2}} \ d\xi \\ &= \frac{1}{\sqrt{2\pi}} \left(\int_{-\infty}^{\xi_0(x_0)} + \int_{\xi_0(x_0)}^{+\infty} \right) u(x_0(\xi_0), \xi) \ \psi_k(\xi) e^{-\frac{\xi^2}{2}} \ d\xi \qquad . \end{aligned} \tag{27}$$

Plugging (25) into the above equation yields

$$\begin{aligned} v_k(x_0) &= \frac{1}{\sqrt{2\pi}} \left(\int_{-\infty}^{\xi_0} (-\sin x_0(\xi_0)) \psi_k(\xi) e^{-\frac{\xi^2}{2}} d\xi + \int_{\xi_0}^{+\infty} \sin x_0(\xi_0) \ \psi_k(\xi) e^{-\frac{\xi^2}{2}} d\xi \right) && (28) \\ &= \frac{\sin x_0(\xi_0)}{\sqrt{2\pi}} \left(\int_{\xi_0(x_0)}^{+\infty} - \int_{-\infty}^{\xi_0(x_0)} \right) \psi_k(\xi) e^{-\frac{\xi^2}{2}} \ d\xi && (29) \\ &= \frac{\sin x_0(\xi_0)}{\sqrt{2\pi}} \left(d_k - 2 \int_0^{\xi_0(x_0)} \psi_k(\xi) e^{-\frac{\xi^2}{2}} \ d\xi \right) , && (30) \end{aligned}$$

where d_k is independent of x_0. The last equality is due to the fact that $\psi_k(\xi)$ is odd (even) function for odd (even) k. Denote the integral in the last expression as $g(x_0)$. Using the chain rule, one can verify

$$\frac{\partial g(x)}{\partial x} = \frac{\partial \xi}{\partial X_s}|_{X_s = x} \quad \psi_k(x) \ e^{-\frac{x^2}{2}} , \tag{31}$$

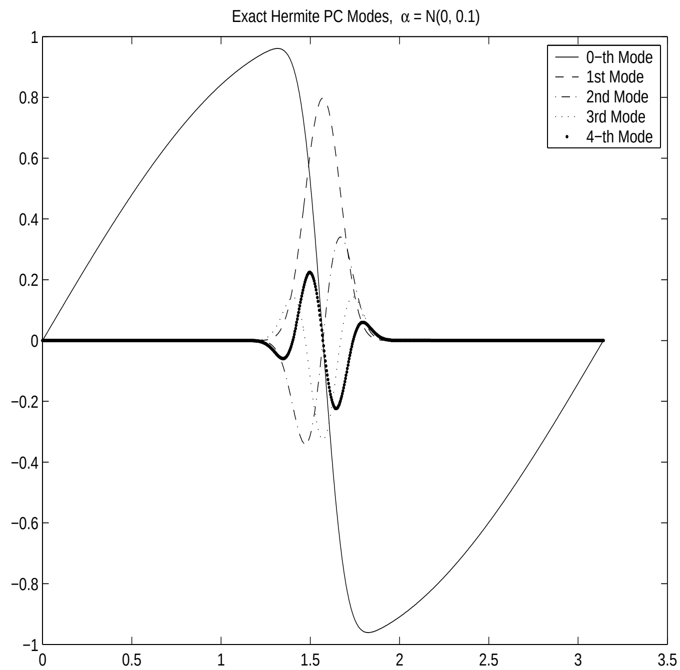

Figure 1: The first five Hermite Polynomial Chaos Modes for the steady state solution of the equation (13) when $\alpha \sim N(0, 0.1)$.

from which one can see that $g(x)$ is a smooth function. The chain rule is valid because ξ is a smooth function of the shock position X_s on $(0, \pi)$ (See (24)). So we have proven that $v_k(x)$ is a smooth function of x for any k. ■

In Fig. 1, we show the first five Hermite polynomial chaos modes for the steady state solution of Eq. (13) when $\alpha \sim N(0, 0.1)$. Figure 2 shows the absolute values of the first 21 PC modes at the points 1.5708 and 1.3959. Note the slow decay due to the discontinuity of the solution in the random space.

To solve numerically equation (13) we seek a solution of the form

$$u_p(x, \beta, t) = \sum_{k=0}^{p} v_k(x, t) \psi_k(\xi).$$

Following the procedure outlined in Sec. 2.2.2 we obtain

$$\frac{\partial v_k}{\partial t} + \sum_{i,j=0}^{p} e_{ijk} \left(\frac{v_i v_j}{2} \right)_x = \delta_{k,0} \left(\sin x \cos x \right) \qquad k = 0, 1, \cdots p \tag{32}$$

where $\delta_{k,0}$ is the Kronecker delta function.

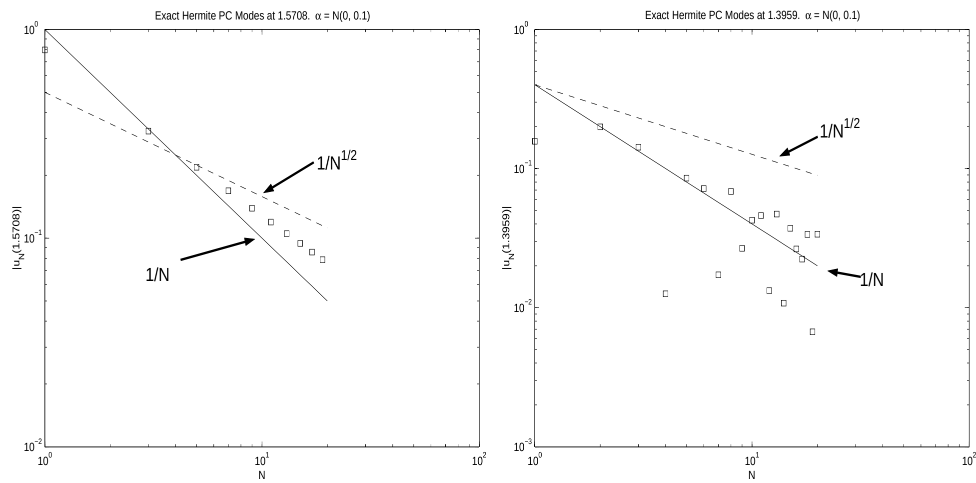

Figure 2: Decay rate of the absolute values (at x) of the first 21 Hermite Polynomial Chaos Modes for the steady state solution of the equation (13) when $\alpha \sim N(0, 0.1)$. Left: at the point $x = 1.5708$; Right: at the point $x = 1.3959$

Remark: For this model problem, we are interested in the statistics of the shock positions which are derived from the solutions. To achieve this we use a Monte Carlo method on the computed solution $u_p = \sum_{k=0}^{p} v_k(x,t)\ \psi_k(\xi)$ of (32). More precisely, we first generate a number of samples of ξ, and compute the realizations of the solution by the expansion. The shock position can then be extracted from each realization. Finally, we can compute the statistics of the shock positions. This procedure is very fast because only the series evaluation is involved in computing each realization.

Numerical Results

Before solving Eq. (32), we check how accurately the PC representation approximates the initial condition. The errors for $\alpha = N(0, 0.1)$ and $N(0, 0.3)$ are plotted in Fig. 3. Spectral accuracy is observed for the PDF-weighted pointwise errors.

We have applied two schemes to solve Eq. (32) : a first order conservative finite difference (FD) scheme with local Lax-Friedrich flux (LLF) ([15]) and a Chebyshev collocation method ([6]) with exponential filtering in space. ([16]). A third-order TVD Runge Kutta scheme ([13]) has been used for the time discretization whenever Chebyshev collocation method is used for the spatial discretization. Otherwise, the first-order forward Euler scheme is used.

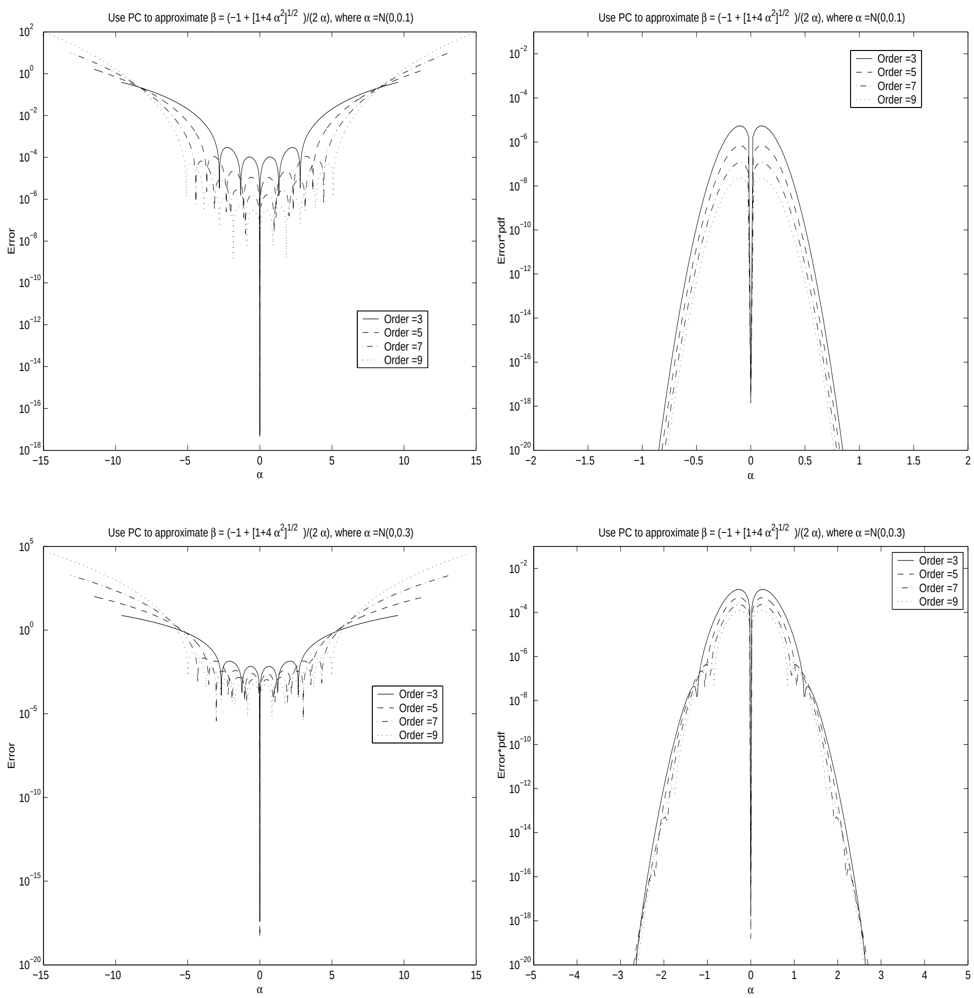

Figure 3: Approximate $\beta = \frac{-1+\sqrt{1+4\alpha^2}}{2\alpha}$ with Hermite Polynomials Chaos expansion. Upper two pictures: $\alpha = N(0, 0.1)$; Lower two pictures: $\alpha = N(0, 0.3)$; Left two : the point wise error; Right two : the product of the point wise error and the PDF.

In all following figures, the 'exact PDF' is from the analytical formula Eq. (22); the 'exact PDF from OSCM' is computed by the OSCM method with a large number (20000 unless otherwise given) of samples. In that case, we first generate samples of β, compute the shock positions from the analytical formula, and then compute the PDF by the OSCM method with those shock positions. The 'p-th order PC' represents the PDF computed by the OSCM method with the same number of shock positions. In this case, however, the shock positions are computed based on the series expansion.

Figure 4 presents the results obtained by the finite difference scheme. The accuracy of the PDF is much worse than that obtained using the Chebyshev collocation method (Fig. 5). The main reason is the large dissipation of the scheme through the local Lax-Friedrich flux which depends on the eigenvalues of the flux-Jacobian of the system. Increasing the number of PC terms in the numerical solution of Eq. (32), increases the size of the system and the spectral radius (as shown in Table 1), and finally leads to additional dissipation. Therefore, only the Chebyshev collocation method with $N = 128$ is used for the spatial discretization in all following numerical tests of the paper. And sixth order filtering is used in space if it is not specified otherwise.

Table 1: Largest absolute eigenvalue (λ) of the flux-Jacobian matrix in Eq. (32). $\alpha = N(0, 0.1)$. 1000 grid points is used in the spatial direction.

PC Order	3	5	7	9	11
λ	3.41	6.95	19.04	29.07	42.24

The errors of up to fourth order moment of the shock position are also computed for the PC method with Chebyshev collocation method for the spatial discretization (See Fig. 6). When $\alpha \sim N(0, 0.1)$, the errors are very small for fifth or higher order PC method. It is consistent with the PDF result in Fig. 5. For $\alpha \sim N(0, 0.3)$ or $N(0, 0.6)$, slow convergence is observed for high order moments. The spatial and time discretization errors dominate when the errors are small, thus the lack of improvement when increasing p.

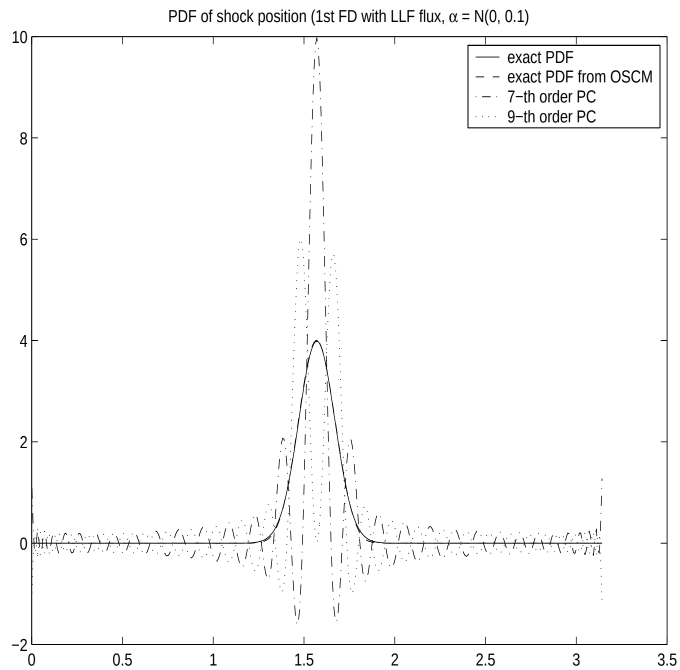

Figure 4: PDF of shock positions from Hermite polynomial chaos methods. $\alpha = N(0, 0.1)$. A first order conservative scheme with local Lax-Friedrich flux is used for the spatial discretization. 1000 grid points on the domain $[0, \pi]$. CFL $= 0.9$.

3.2 Inhomogeneous Random Initial Condition II: Jacobi Chaos

In this section we consider the initial condition (17) with β being a Beta random variable ($\beta \sim \text{Beta}(r, s)$) over the domain $[-1, 1]$. For this initial random process, Jacobi polynomials are the natural choice for the PC basis functions ([18]).

The PDF of the shock locations X_s is

$$p(X_s) = \frac{(1+\beta)^{r-1}(1-\beta)^{s-1}}{2^{r+s-1}B(r,s)} \sin X_s \ , \qquad\qquad 0 < X_s < \pi \ , \tag{33}$$

where $\beta = -\cos(X_s)$, $B(r, s) = \frac{\Gamma(r)\Gamma(s)}{\Gamma(r+s)}$ is the beta function, and $\Gamma(r)$ is the Gamma function.

Similar to the Hermite polynomials chaos case, it is enough to use the one-dimensional Jacobi chaos. The equations resulting from applying the Galerkin procedure have the same form (32), but with the matrix e being computed from Jacobi polynomials instead of Hermite polynomials.

As before we can state

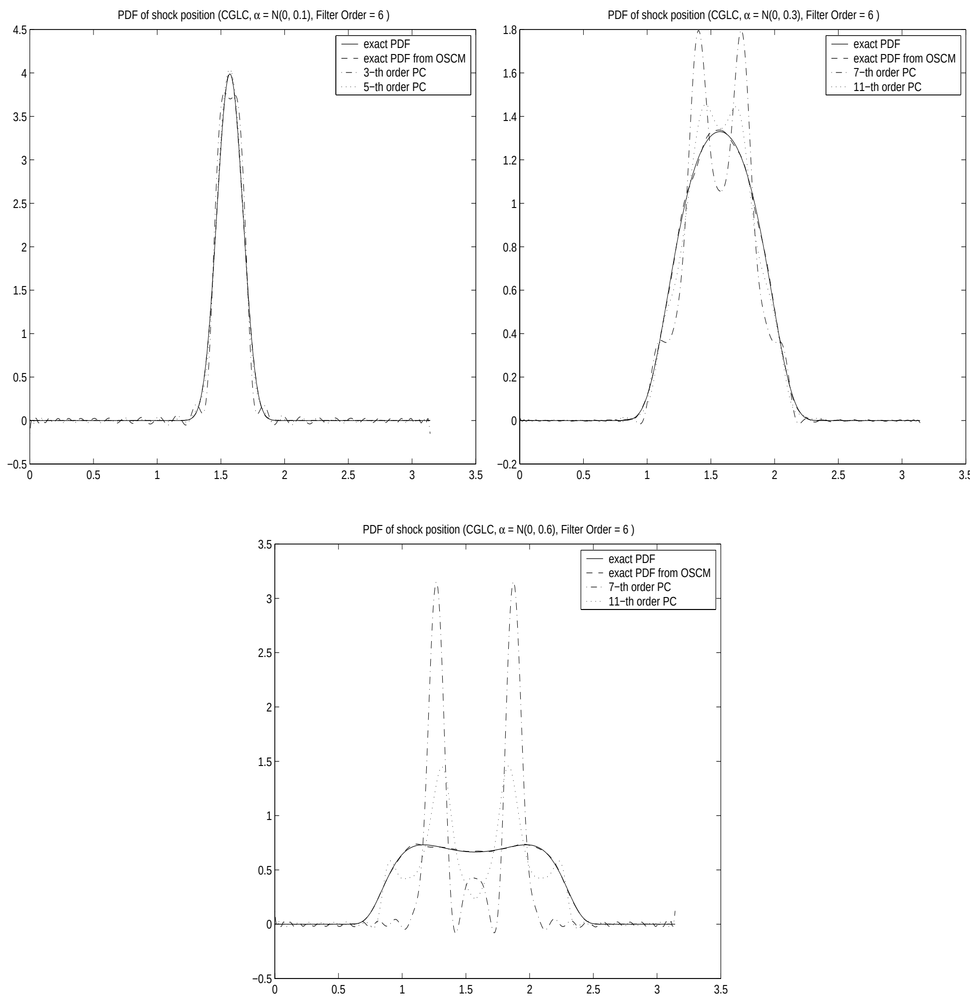

Figure 5: PDF of shock positions from Hermite polynomial chaos methods. A Chebyshev collocation method with $N = 128$ is used for the spatial discretization. $\Delta t = \frac{2}{3p} N^{-2}$, where p is the order of polynomial chaos. Exponential filter order is 6. Upper Left: $\alpha = N(0, 0.1)$, 100000 samples are used to compute the PDF by the OSCM method; Upper right: $\alpha = N(0, 0.3)$, 100000 samples are used to compute the PDF by OSCM; Lower left: $\alpha = N(0, 0.6)$, 200000 samples are used to compute the PDF by OSCM.

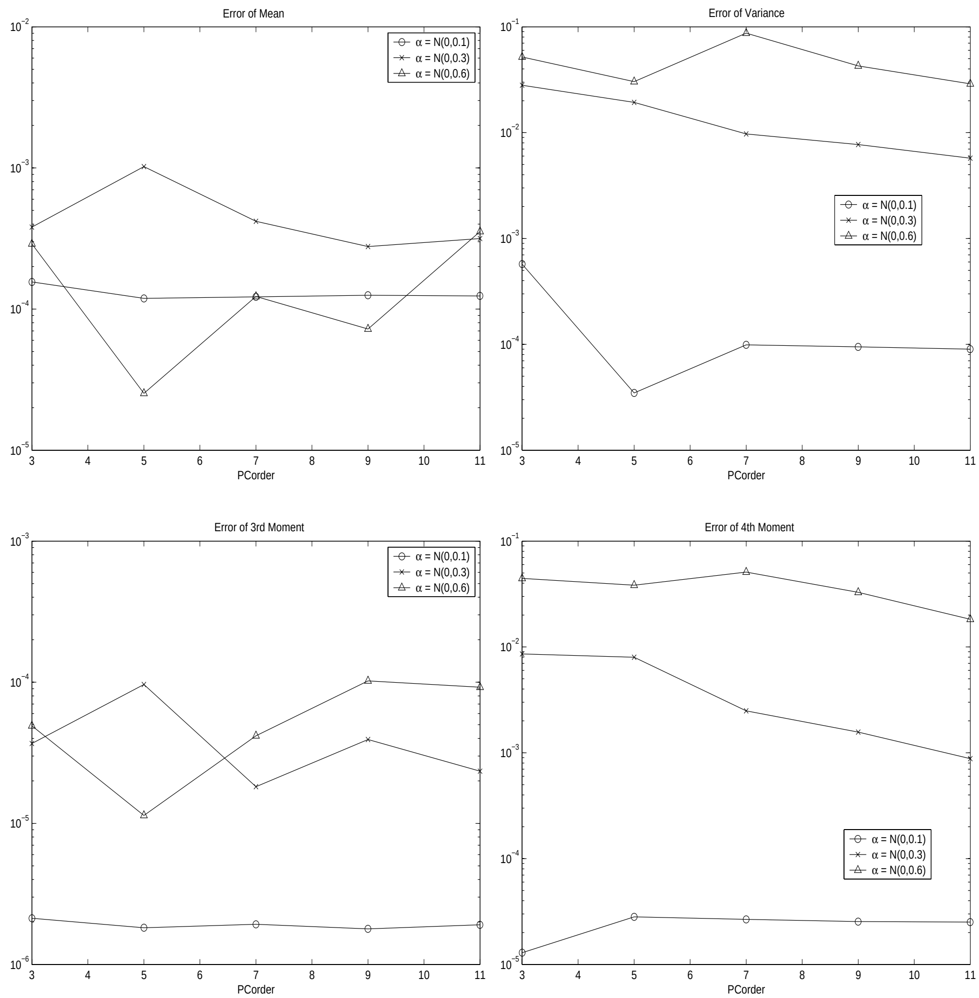

Figure 6: Errors of up to fourth moment of the shock position whose PDF is shown in Fig. 5. Upper left: mean; Upper right: variance; Lower left: 3rd moment (skewness); Lower right: 4th moment (kurtosis). '-∘': $\alpha \sim N(0, 0.1)$; '-x': $\alpha \sim N(0, 0.3)$; '-△': $\alpha \sim N(0, 0.6)$.

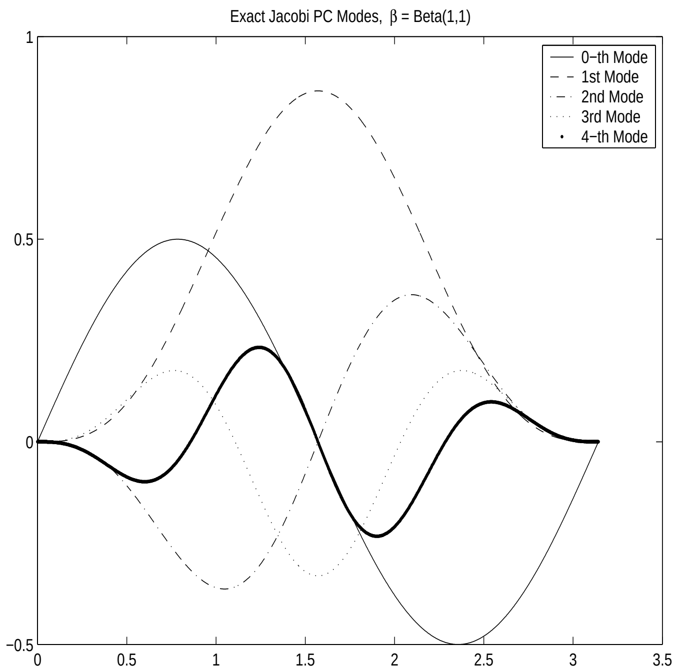

Figure 7: The first five Jacobi polynomial chaos modes, also called Legendre chaos modes because $r = s = 1$. $\beta \sim \text{Beta}(r, s)$ on $[-1, 1]$.

Theorem 3 *(Smoothness) The coefficients in the Jacobi polynomial chaos expansion of the steady state solutions are smooth.*

Proof: The proof is omitted as it follows the approach in Theorem 2. ■

In Fig. 7-10, we show the first five Jacobi polynomial chaos modes and the decay rate of the first 21 PC modes at some points for $r = s = 1$ and $r = s = 10$.

Numerical Results

For this case, as β is Beta distributed, there is no error introduced when expanding the initial condition into Jacobi polynomial chaos basis functions. We test three different initial conditions: $\beta \sim \text{Beta}(1,1), \text{Beta}(5,5)$ and $\text{Beta}(10,10)$. The results from the Chebyshev collocation method are shown in Fig. 11. When $\beta \sim \text{Beta}(10,10)$, the PDF is computed with high accuracy. As the variance of β increases, many more PC terms are needed to produce reasonable results. This is because the solution is discontinuous in the random space and β is more localized for large r (Note that β has PDF $\sim (1-\beta^2)^r$ when $r = s$).

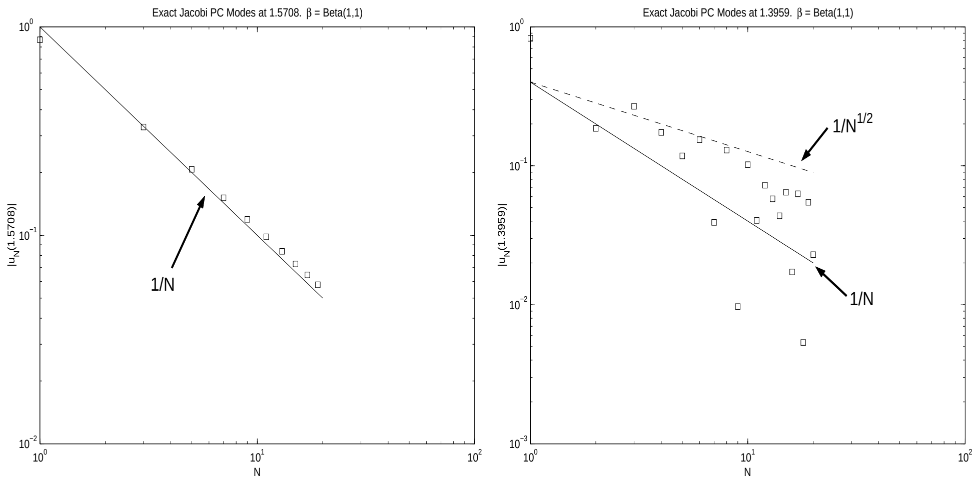

Figure 8: Decay rate of the absolute values (at x) of the first 21 Jacobi polynomial chaos modes. $\beta \sim \text{Beta}(r, s)$ on $[-1, 1]$. Left: at the point $x = 1.5708$; Right: at the point $x = 1.3959$

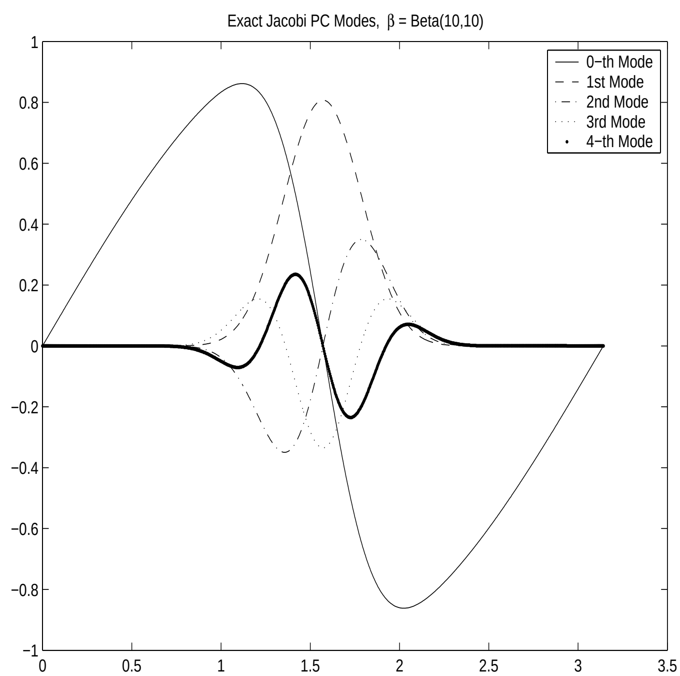

Figure 9: The first five Jacobi polynomial chaos modes, $r = s = 10$. $\beta \sim \text{Beta}(r, s)$ on $[-1, 1]$.

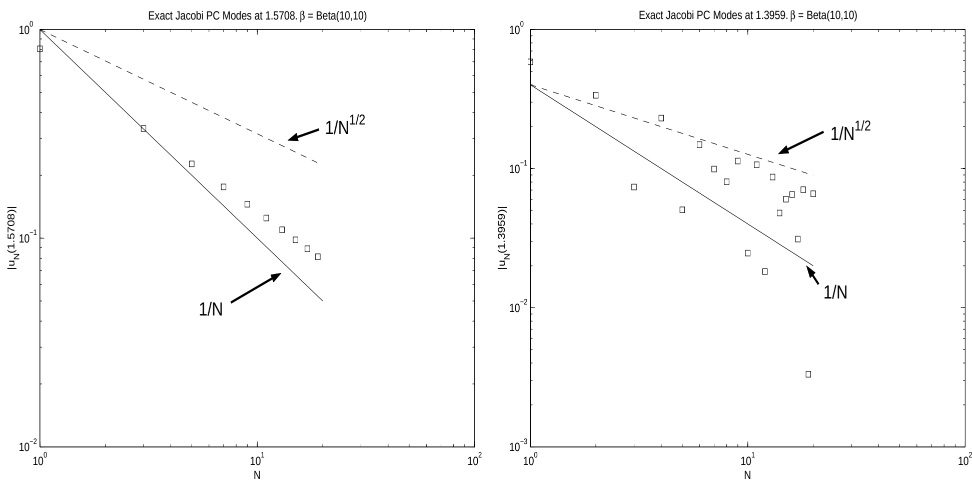

Figure 10: Decay rate of the absolute values (at x) of the first 21 Jacobi polynomial chaos modes, $r = s = 10$. $\beta \sim \text{Beta}(r, s)$ on $[-1, 1]$. Left: at the point $x = 1.5708$; Right: at the point $x = 1.3959$

3.3 Initial Condition III: Hermite Chaos

In this section we consider random *field* initial conditions of the form:

$$u(x, \beta, t = 0) = \sigma(\sqrt{\lambda_1} f_1(x)\beta_1 + \sqrt{\lambda_2} f_2(x)\beta_2) \,, \tag{34}$$

where β_1 and β_2 are functions of two *iid* Gaussian random variables α_1 and α_2 respectively. The relations between α_i and β_i are given in (18).

The constants λ_1, λ_2 are the first two eigenvalues and $f_1(x)$ and $f_2(x)$ are the first eigenfunctions of the KL expansion for the exponential correlation:

$$C(x_1, x_2) = e^{-|x_1 - x_2|/10} \,, \tag{35}$$

Figures 12 and 13 show the PDF of the shock positions for $\alpha_1, \alpha_2 \sim N(0, 0.1)$ and $N(0, 0.3)$ when $\sigma = 0.4$.

3.4 Initial Condition IV: Jacobi Chaos

As in Sec. 3.3, the initial condition has the exponential correlation (35). But instead, we assume β_1 and β_2 have Beta distribution in the final numerical initial condition (34). Numerical results for $\beta_1, \beta_2 \sim \text{Beta}(5, 5)$ and $\text{Beta}(10, 10)$ are shown in Fig. 14 and 15.

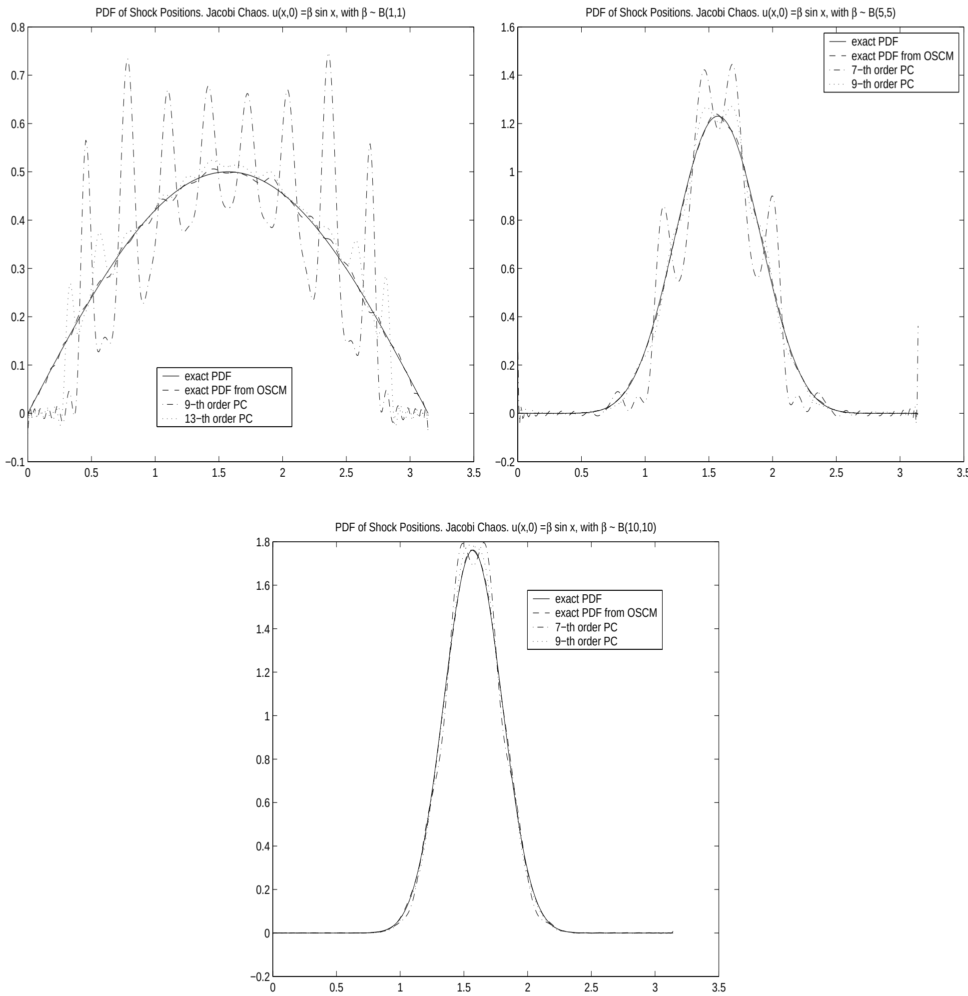

Figure 11: PDF of shock positions from Jacobi polynomial chaos methods. 100000 samples are used to compute the PDF by the OSCM method. Other parameters are the same as used in Fig. 5. Upper left: $\beta = \mathrm{Beta}(1,1)$; Upper right: $\beta = \mathrm{Beta}(5,5)$; Lower: $\beta = \mathrm{Beta}(10,10)$.

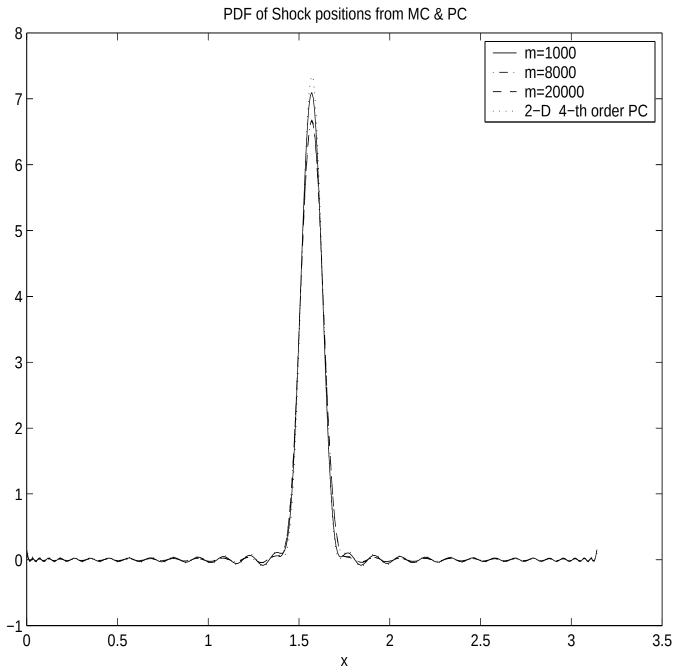

Figure 12: PDF from MC with 1000, 8000, 20000 samples and 2D 4th order Hermite chaos method. $\Delta t = N^{-1.5}$ for MC methods. $\Delta t = \frac{2}{3\frac{(n+p)!}{n!p!}} N^{-1.5}$ for PC methods. 20000 samples are used to compute the PDF for the PC method with the OSCM method. $\sigma = 0.4$. $\alpha_1, \alpha_2 \sim N(0, 0.1)$.

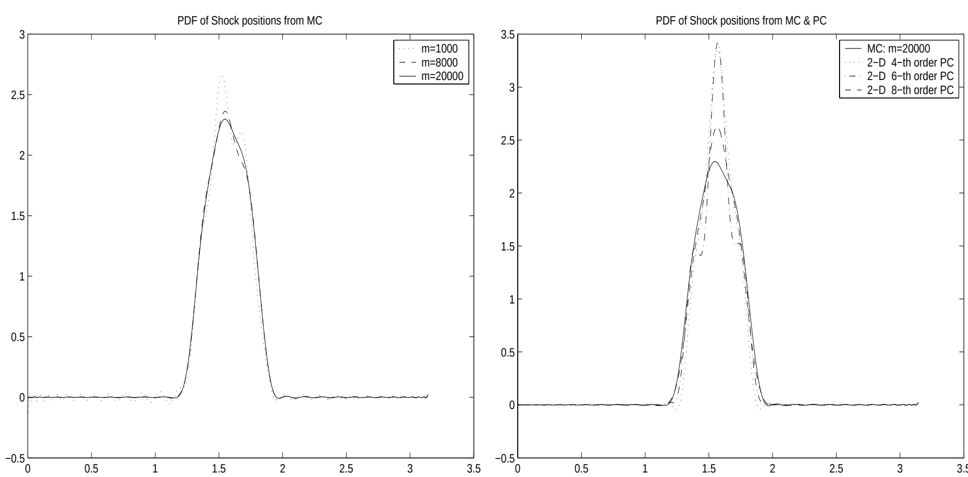

Figure 13: PDF of shock positions. $\alpha_1, \alpha_2 \sim N(0, 0.3)$. All other parameters are the same as used in Fig. 12. Left: Monte Carlo method with 1000, 8000, 20000 samples; Right: 4,6,8-th order Hermite chaos.

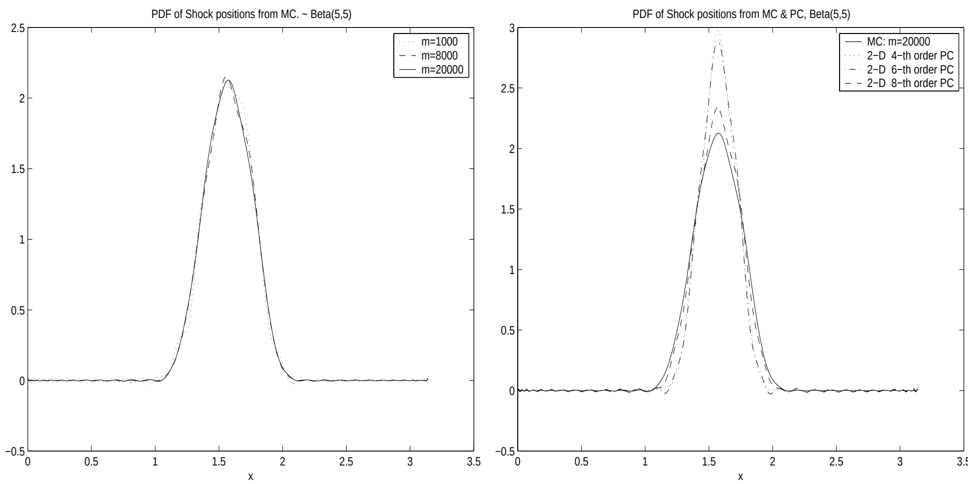

Figure 14: PDF of shock positions. $\beta_1, \beta_2 \sim \text{Beta}(5,5)$. All other parameters are the same used in Fig.12. Left: Monte Carlo method with 1000, 8000, 20000 samples; Right: 4, 6, 8th-order Jacobi chaos.

One can see that the PDF from polynomial chaos methods does converge to the exact PDF, although it is still not very accurate for the eighth-order Jacobi chaos.

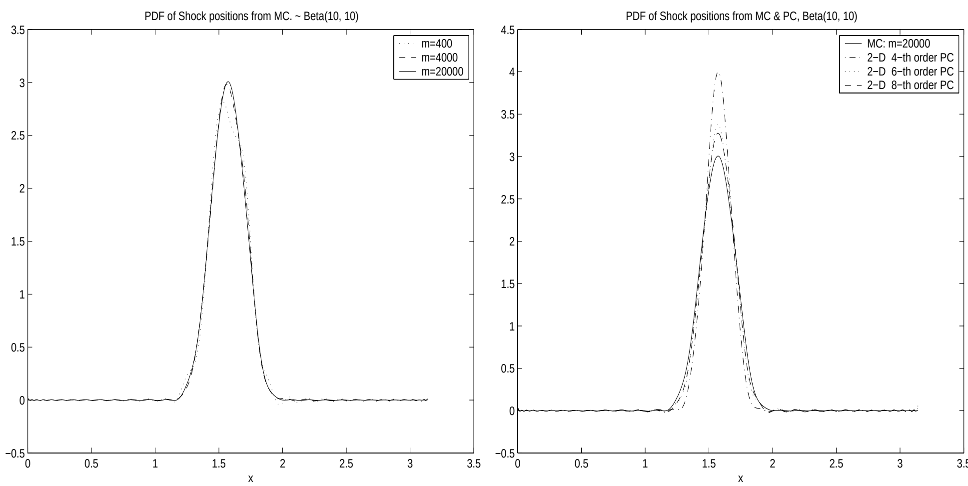

Figure 15: PDF of shock positions. $\beta_1, \beta_2 \sim \mathrm{Beta}(10, 10)$. All other parameters are the same as used in Fig.12. Left: Monte Carlo method with 400, 4000, 20000 samples; Right: 4, 6, 8th-order Jacobi chaos.

4 Summary

We have studied the effect of random initial conditions on the structure of the steady state isentropic flow in a dual-throat nozzle with equal throat areas. Generalized polynomial chaos methods were implemented to analyze the uncertainty of the shock position for different stochastic initial conditions. Our main conclusions are:

- The polynomial chaos expansion modes are smooth functions of the spatial variable x, although the individual solution realizations are discontinuous in the spatial variable x.

- The solution is discontinuous in the random variable space at a fixed point x. Filtering is necessary for the stability of the scheme, as generalized polynomial chaos methods are spectral representations of the random processes.

- When the variance of the initial condition is small, the probability of the density function (PDF) of the shock locations is computed with high accuracy. Otherwise, many PC expansion terms are needed to produce reasonable results. As first noted by Chorin, this is due to the slow convergence of PC expansions of discontinuous functions in the random fields.

- The largest absolute eigenvalue of the flux-Jacobian matrix of the system increases quickly with respect to the number of PC terms used in the expansion. This might cause large dissipation for some numerical schemes. The increasing size of the system, when using more PC terms, could also be problematic if one wants to solve the system with a high order numerical scheme using characteristic decomposition, e.g., high order ENO or WENO.

Acknowledgment The authors thank Prof. Chorin (UC Berkeley) for his many valuable comments on Hermite chaos methods. We would also like to thank Prof. Chauviere (Univ. Blaise Pascal, France) for his useful suggestions. The work of the second author was supported by AFOSR grant F49620-02-1-0113 and DOE grant DE-FG02-98ER25346. The work of the last author was partly supported by an NSF Career Award contract DMS-0132967, ARO under contract DAAD19-01-1-0631 and by the Alfred P. Sloan Foundation through a Sloan Research Fellowship.

References

[1] R. Askey and J. Wilson, *Some Basic Hypergeometric Polynomials that Generalize Jacobi Polynomials*, Memoirs of the American Mathematical Society, AMS, Providence, RI, 319, 1985.

[2] A. Chorin, *Gaussian Fields and Random Flow*, Journal of Fluid Mechanics 63 (1974), pp. 21-32.

[3] C.M. Dafermos, *Trend to Steady State in a Conservation Law with Spatial Inhomogeneity*, Quarterly of Applied Mathematics, vol. XLV, no. 2 (1987).

[4] D. Funaro , *Polynomial Approximation of Differential Equations.* Lecture Notes in Physics, m 8. Springer Verlag, Berlin. 1992.

[5] R. Ghanem And P. D. Spanos, *Stochastic Finite Element: A Spectral Approach* Springer-Verlag, New York, 1991.

[6] D. Gottlieb, S.A. Orszag, *Numerical Analysis of Spectral Methods: Theory and Applications*, CBMS-NSF Regional Conference Series in Applied Mathematics (SIAM, Philadelphia, 1977).

[7] Luc Huyse and Robert W. Walters *Random Field Solutions Including Boundary Condition Uncertainty for the Steady-state Generalized Burgers' Equation*, ICASE Report 2001-35/ NASA CR-2001-211239, 2001

[8] Richard M. Jendrejack, Juan J. de Pablo and Michael D. Graham *A Method for Multi-Scale Simulation of Flowing Complex Fluids.* J. Non-Newtonian Fluid Mech. 108 (2002) 123-142

[9] M. Loève, *Probability Theory*, Fourth edition, Springer-Verlag, 1977.

[10] W. L. Oberkampf, J. C. Helton, and K. Sentz *Mathematical Representation of Uncertainty*, AIAA-paper 2001-1645, in 42^{nd} AIAA/ASME/ASCE/AHS/ASC Structures, Structural Dynamics, and Materials Conference and Exhibit, Seattle, WA, 2001.

[11] M.D. Salas, S. Abarbanel and D. Gottlieb *Multiple Steady States For Characteristic Initial Value Problems.* Applied Numerical Mathematics 2(1986) 193-210.

[12] G. I. Schuëller (Editor) *A State-of-the-art Report on Computational Stochastic Mechanics*, Probabilistic Engineering Mechanics, Vol. 12, No.4, pp. 197-321, IASSAR report, 1997.

[13] C.-W. Shu, *A Survey of Strong Stability Preserving High Order Time Discretizations*, in Collected Lectures on the Preservation of Stability under Discretization, D. Estep and S. Tavener, editors, SIAM, 2002, pp.51-65.

[14] B. Sudret, and A. Der Kiureghian, *Stochastic Finite Element Methods and Reliability: A state-of-the-art report*, Report No. UCB/SEMM-2000/08, Department of Civil & Environmental Engineering, University of California, Berkeley, CA, November, 2000.

[15] Eleuterio F. Toro *Riemann Solvers and Numerical Methods for Fluid Dynamics: a practical introduction.* Berlin, New York, Springer, 1997.

[16] Hervé Vandeven *Family of Spectral Filters for Discontinuous Problems.* Journal of Scientific Computing, Vol. 6, No. 2, 1991

[17] Robert W. Walters and Luc Huyse *Uncertainty Analysis for Fluid Mechanics with Applications* ICASE Report 2002-1/ NASA CR-2002-211449, 2002

[18] D. Xiu and G. E. Karniadakis *Modeling Uncertainty in Flow Simulations via Generalized Polynomial Chaos*, Journal of Computational Physics, 2001.

[19] A. M. Yaglom *An Introduction to The Theory of Stationary Random Functions*, NJ, Prentice-Hall (1962)